

A capacitive probe for measuring the clearance between the piston and the cylinder of a gas piston gauge

Walter J. Bowers and Douglas A. Olson

National Institute of Standards and Technology, 100 Bureau Drive, MS 8364, Gaithersburg, Maryland 20899, USA

(Received 17 November 2009; accepted 17 January 2010; published online 10 March 2010)

We used a capacitive technique to determine the radial clearance between the piston and cylinder of a gas piston gauge. This method determines the effective area of a piston gauge pressure standard, independent of calibration against another piston gauge or manometer, as long as the diameter of the piston is dimensionally measured. It also allows an independent determination of piston gauge distortion due to pressure. We have used this technique to measure the clearance and the distortion of six gas piston gauges of the Ruska 2465 type operating in gauge mode. Measurements were made on two gauges each in the low, middle, and high ranges. We describe the capacitance technique and the results of the measurements on the six piston gauges. [doi:10.1063/1.3310092]

I. INTRODUCTION

A simple piston gauge generates pressure, p , in a fluid by applying a known force, F , to a known area ($p=F/A$). The force is supplied by a known mass acting under gravity, pushing a piston into a closed cylinder. The piston is marginally smaller than the cylinder and fluid fills the gap between the two components. The pressure acts on the “effective area,” A_e , rather than the piston’s cross-sectional area, as vertical forces in the gap due to the fluid add to the normal force at the bottom of the piston. In the limit when the gap is small compared to the piston diameter, along with both a straight and round piston and cylinder, it can be shown that the effective area is equal to the average of the piston and cylinder area.¹ Using A_e as the “calibration factor” to account for all the fluid-related forces on the piston gauge, the pressure can be expressed as

$$p = \frac{\sum_i m_i g \left(1 - \frac{\rho_a}{\rho_{mi}}\right)}{A_e}, \quad (1)$$

where m_i are the masses of the weights loaded onto the piston with densities ρ_{mi} , g is the local acceleration of gravity, and ρ_a is the density of gas surrounding the masses (in gauge mode, air at atmospheric pressure). In Eq. (1), p is the gauge mode pressure. In most cases, A_e is determined by comparison to pressures generated by a manometer or another piston gauge. Due to distortion under pressure and thermal expansion of the materials making up the piston and cylinder, A_e is a function of both temperature and pressure. A common expression for the pressure dependence is

$$A_e = A_0(1 + b_1 p + b_2 p^2), \quad (2)$$

with A_0 as the area of the gauge at zero pressure and at a reference temperature (NIST uses 23 °C). b_1 is a linear distortion coefficient and b_2 is a quadratic distortion coefficient. Changes in area as the temperature departs from the

reference temperature are accounted for by applying coefficients of thermal expansion for the piston and cylinder.

The combination of relative simplicity of operation and reasonable cost has made the gas piston gauge a useful transfer standard linking the primary pressure standards to several types of pressure measurement devices. Primary standards can be mercury manometers or other piston gauges whose piston and cylinder diameters have been carefully measured.² At NIST, low pressure range (large diameter) piston gauges are used to calibrate successively higher range (smaller diameter) piston gauges, extending to a pressure of about 17 MPa (2500 psi).³ The b_2 coefficient can be taken as zero for most piston gauges operating at pressures below 17 MPa.

A piston gauge could be characterized as a primary pressure standard (i.e., without comparison to another pressure standard) if the piston and cylinder diameters could be measured over the operating range of pressure. At NIST, two gas piston gauges, each 36 mm diameter and operating to 1 MPa, are characterized as primary standards.² State of the art dimensional measurements can determine the diameter and straightness of pistons with an expanded uncertainty of 50 nm or less.^{2,4} Dimensional measurement of the cylinder is more difficult, especially with bore diameters less than 20 mm. Present coordinate measuring machines operate at atmospheric pressure; so to characterize a piston gauge as a primary standard above atmospheric pressure, the distortion with pressure is modeled. For piston gauges designed for higher operating ranges, diameters are smaller, the uncertainties of the distortion models are more significant, and it becomes impractical to measure the cylinder bore diameters.

If the radial clearance between the piston and cylinder (h , where $h=r_c-r_p$, r_c is the cylinder radius, and r_p is the piston radius) could be measured, the effective area of a piston gauge could be estimated without measuring the cylinder bores. The average clearance gap between a piston and its cylinder along its length of engagement is typically between 0.4 and 2.0 μm , with the cylinder tapered slightly

larger at both ends (bell mouthed) and the piston tapered slightly smaller at either one or both ends or not at all.

In this paper we propose a method for measuring the capacitance of the gap between a piston and cylinder that is used as a pressure standard. This method has been used in previous studies at NIST; however, the measurement principles and uncertainties were not described.^{5,6} A capacitive method was applied to an oil piston gauge in Ref. 7; because the relative dielectric permittivity of the oil was not well known, the gap width calculated from the capacitance measurements is more uncertain than that calculated with a gas piston gauge. From modeling of how the capacitance depends on characteristics of the gap and the gas that fills it, we can determine a characteristic gap width. With the combination of a relatively large area and a small gap in the piston/cylinder capacitor, the change in gap with pressure can be related to the change in capacitance as a function of pressure. This technique can be used from atmospheric pressure up to the full pressure of the piston gauge, providing a method for determining piston-cylinder distortion that does not require comparison to another piston gauge. Precise knowledge of piston and cylinder diameters is not required to measure the distortion of the cylinder relative to the piston. This method has been applied to commercially available gas piston gauges, of the Ruska⁸ 2465 type.

II. CAPACITIVE METHOD

For two long concentric cylinders with negligible end effects and uniform radial clearance, the familiar capacitance equation can be rearranged to solve for the clearance, h , as

$$h = \frac{D}{2} [e^{2\pi K \epsilon_0 L / C_g} - 1], \quad (3)$$

where h is the clearance gap between the concentric plates (piston and cylinder), D is the piston diameter, L is the piston/cylinder engagement length, C_g is the capacitance of the gap, K is the relative permittivity of the gas in the gap, and ϵ_0 is the electric permittivity constant or $\epsilon_0 = 8.854 \times 10^{-12}$ F/m.

Since $h/D \ll 1.0$, this can be simplified with no loss in accuracy to

$$h = \frac{\pi D L K \epsilon_0}{C_g}. \quad (4)$$

For the Ruska low, middle, and high range pistons, $L = 43$, 27, and 23 mm, respectively, and $D = 20.7$, 10.3, and 3.27 mm for the same pistons. K is pressure and temperature dependent and has recently been reported.⁹ Using the coefficients of the polynomial expansion given in Ref. 9, at 23 °C, K is given for nitrogen by

$$K = 1 + 5.3457 \times 10^{-9} p - 1.079 \times 10^{-18} p^2 + 1.2513 \times 10^{-24} p^3, \quad (5)$$

where p is the absolute pressure in pascals. For nitrogen, K ranges from 1.000 535 at 100 kPa to 1.037 796 at 7 MPa. The correlation has a standard uncertainty of about 3×10^{-5} times the coefficient on the linear term in pressure, or at 7 MPa the uncertainty in K is about 1×10^{-6} . A larger com-

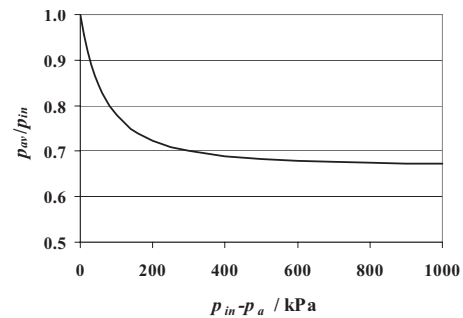


FIG. 1. Ratio of average gap pressure to inlet pressure (p_{av}/p_{in}) in a constant width gap as a function of pressure difference ($p_{in} - p_a$) between gap inlet and ambient (gap exit). Shown for $p_a = 101$ kPa.

ponent of uncertainty in K is the choice of the pressure to use in Eq. (5). In the clearance region between the piston and cylinder, the pressure will vary from the system pressure at the bottom of the piston (gap inlet), to atmospheric pressure at the exit of the gap. The gas permittivity in the gap will vary with position due to the pressure gradient; hence even if the gap width was constant, the local capacitance per unit area will vary with position. In order to apply Eq. (4) with a single value of K , we calculate a pressure distribution in the gap assuming constant width, viscous flow, and the perfect gas equation of state. This yields a pressure profile that varies with the square root of the position from the gap inlet. Integrating this profile over the gap length yields an average pressure given by

$$p_{av} = \frac{2}{3} p_{in} \frac{\left[1 - \left(\frac{p_a}{p_{in}} \right)^3 \right]}{\left[1 - \left(\frac{p_a}{p_{in}} \right)^2 \right]}. \quad (6)$$

Here, p_{in} is the pressure at the gap inlet and p_a is the atmospheric pressure at the gap exit (both expressed as absolute pressures). Equation (6) is shown graphically in Fig. 1 for the case when $p_a = 101$ kPa, with $p_{in} - p_a$ on the x -axis plotted up to 1000 kPa. For pressures above 1000 kPa, $p_{av}/p_{in} = 2/3$. K is calculated using p_{av} for pressure, which is then substituted in Eqs. (5) and (4) to yield h . In the results that follow we assume constant pressure, constant gas permittivity, and constant capacitance per unit area in determining h using Eq. (4).

III. EXPERIMENTAL SETUP

We have used the piston as a probe, i.e., plate 1 of a capacitor in Fig. 2 with the cylinder as plate 2. The capacitance bridge used in our measurement was a Stanford Research System model SR715 LCR. The electrical connection to plate 1 was made via a fine copper wire suspended into a pool of mercury contained in a brass jig; the jig was attached by friction to the top of the mass stack. The mercury pool allows maintaining the electrical circuit during relative movement between piston and cylinder. The connection to plate 2 was made with a screw on the base plate. The calibration of this bridge was verified prior to the present measurements and checked frequently thereafter with a set of four very stable, calibrated capacitors provided by the

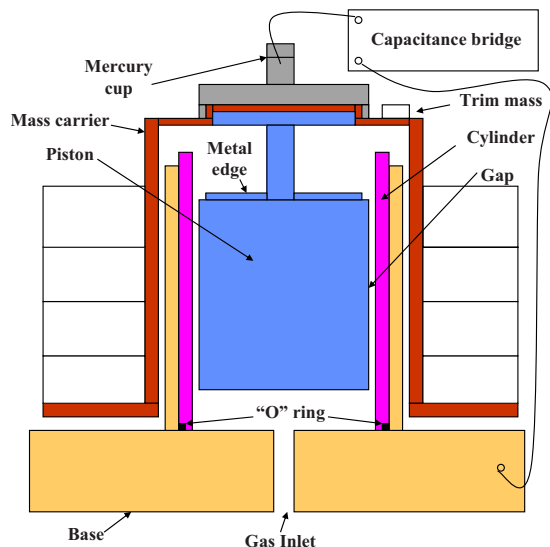


FIG. 2. (Color online) View of capacitance circuit utilizing a gas piston gauge.

Electricity Division at NIST. The values of these capacitors were 9916.4, 5108.7, 479.3, and 39.81 pF at 1 kHz. The relative standard uncertainty of the calibrated capacitors was 5×10^{-5} (50 ppm). The LCR meter was always used at 1 kHz and measured these same capacitors at 9916.9, 5109.4, 477.89, and 39.075 pF, respectively. For the three piston gauge ranges measured, the capacitance values ranged from high (17 106 pF) to low (5862 pF). Measured background values varied between 200 and 4 pF. Capacitance values of less than 2 pF caused the meter to read “out of range.”

The total capacitance measured by the bridge, C_T , consists of the capacitance of the piston/cylinder gap, C_g , plus the capacitance of other conductors that are in electrical contact with the two “plates” of the capacitor. These additional sources of capacitance are referred to as “stray capacitance,” C_s . Thus, the capacitance of the gap is

$$C_g = C_T - C_s. \quad (7)$$

There are several sources of the stray capacitance. The contributions to the stray capacitance depended on the piston gauge geometries (low, middle, and high), shown in Fig. 3. For the low range piston (20 kPa to 0.3 MPa), we first measured the stray capacitance due to the mass loads only, which was height dependent. We fabricated nonmetallic spacers to suspend the mass loads at several appropriate vertical positions above the cylinder without a piston, and measured the capacitance. Additionally, the stray capacitance was calculated from the small metal vertical edge at the top end of the piston (Fig. 2), which is not part of the gap. The horizontal ends (top and bottom) of the piston have a capacitance with respect to the vertical cylinder. A metal jig was constructed to simulate both ends of the piston and was suspended in the cylinder to measure that capacitance contribution.

The stray capacitance for the other two gauge geometries was measured in similar fashion, especially the contribution from the mass loads. However, in the case of the midrange gauge (30 kPa to 1.4 MPa), a metallic cylinder with insulating rings was used to simulate the stray capacitance from the

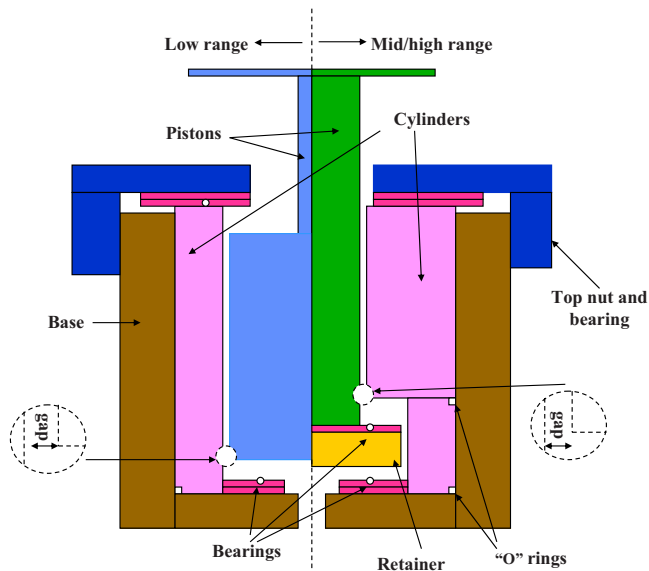


FIG. 3. (Color online) Schematic of piston gauge geometry for Ruska low, middle, and high range pistons.

piston and bearing hardware (shown on the right side of Fig. 3). The stray capacitance for the high range gauge (400 kPa to 7 MPa) was measured with an insulating cylinder equipped with metallic ends.

For the low range gauge (shown in the left side of Fig. 3) the piston is shorter than the cylinder. The piston surface is always completely contained in and capacitively engaged with the cylinder with the deviations from cylindricity (200 nm) being small compared to the size of the capacitor gap (1500 nm). The length of the piston surface is the same regardless of the vertical location of the piston. As the piston drifts down from the top of the cylinder to the bottom, it capacitively couples with a constantly changing cylinder surface. Thus the piston becomes a probe using the recorded capacitance values to map the cylinder dimensional profile. In the cases of the middle and high range gauges, it is the cylinder whose surface remains the same while the piston surface changes with vertical motion.

Although gas piston gauges are operated with rotating pistons and masses when used as pressure standards, such rotation produces large fluctuations (100 pF or more) in capacitance measurements. In the present technique, we have made measurements with nonrotating pistons and eliminated other alignment effects that changed the capacitance. Operating near the top of the pressure range produces stable capacitance readings more quickly, hence the following method was first performed at the high pressure. The centered piston in its cylinder yields the lowest capacitance at any piston height so the alignment height was chosen to be the center of the vertical operating range or “zero” level. One or more strips of paper attached to metal weights provided just enough tangential friction between the piston masses and the base to keep the piston from spontaneously rotating. This is important because even a small variation in the piston and cylinder surface alignment can result in significant differences in capacitance. At the beginning stage of alignment, for the low range gauges, changes of 2000 pF of capacitance

TABLE I. Dimensions, operating conditions, capacitance measurements, and calculated gap clearance for six NIST gas piston gauges. Standard uncertainty listed for gap capacitance and gap clearance. Both h and $u(h)$ assume that gap is uniform in angular and vertical directions.

Piston gauge	L (mm)	D (mm)	$p_{in}-p_a$ (kPa)	C_T (pF)	C_s (pF)	C_g (pF)	$u(C_g)$ (pF)	h (nm)	$u(h)$ (nm)
PG28	42.4	20.68	23.8	16 523	127.2	16 396	16.8	1488.4	2.3
			161.8	16 476	127.2	16 349	16.8	1493.3	2.4
PG29	42.7	20.68	58.3	17 106	89.3	17 017	14.5	1445.0	2.1
			162.1	17 060	89.3	16 971	14.5	1449.4	2.2
PG34	27.4	10.34	80.8	10 611	54.5	10 556	9.4	746.6	1.5
			1392.5	10 410	57.7	10 352	9.4	764.8	2.2
PG37	27.4	10.34	77.9	8479	54.5	8424	8.4	955.8	2.0
			670.3	8425	57.7	8367	8.4	964.8	2.3
PG13	22.8	3.268	2773.9	6051	45.6	6006	6.8	349.2	1.6
			6930.0	5862	45.6	5816	6.8	365.9	3.6
PG35	22.8	3.268	703.2	6418	45.6	6372	4.1	326.7	0.9
			6930.5	5949	45.6	5903	4.1	360.5	3.5

could result from 180° of piston rotation. The rotational alignment of the piston relative to the cylinder was chosen for minimum capacitance at the outset, marked and maintained as precisely as possible throughout the alignment process.

Having found this first minimum, an arbitrarily small movable trim mass, e.g., 2 g, was placed on each of four points (north, south, east, and west) on top of the mass stack at right angles to one another and at the same distance from the center of mass. The capacitance was recorded in each case as the piston drifted down through the zero level. These four values were compared to find the location for the trim mass that “balanced” the mass load and achieved another minimum in the capacitance. Eventually the location was selected such that any change in the trim mass position or in the rotational orientation of the piston caused an increase in capacitance. The gauge was then recharged with gas and the capacitance versus vertical position map was recorded as the piston drifted from the top of the operating range to the bottom. Several scans were taken to evaluate noise and reproducibility. Typically capacitance values for successive drifts through zero were repeated within 1 pF, barring temperature changes or rotational orientation drift.

Each capacitance value, having been adjusted for the aforementioned stray capacitance, represented an integration over the entire area of the piston/cylinder interface. Two Ruska piston gauges in each of three pressure ranges were measured in this way. Low range (0.3 MPa full scale) gauges were designated PG28 and PG29, midrange (1.4 MPa full scale) gauges were PG34 and PG37, and high range (7 MPa full scale) gauges were PG13 and PG35. The capacitance of each gauge was measured at a range of pressures, from which their b_1 (distortion) coefficients can be determined (analysis to follow).

IV. RESULTS OF THE MEASUREMENTS

The measurements of total capacitance, stray capacitance, calculation of gap capacitance, and calculation of gap width for the six piston gauges are summarized in Table I. For each gauge, the measurements and calculations are listed at the lowest and highest gauge pressures tested ($p_{in}-p_a$);

additional measurements were made throughout the pressure range. Note the significant difference in the stray capacitance values for PG28 and PG29, which are of the same nominal design. This is due to the significant difference in size, for the two piston gauges, of the metal edge (shown in Fig. 2) between the tungsten carbide piston surface and the stem portion of the piston that supports the mass load. As the operating pressure range increases for the three designs (low to middle to high), the size of the gap decreases. Smaller gaps at higher pressures keep the fall rates reasonably low.

A typical trace of gap capacitance as a function of vertical position is shown in Fig. 4 for PG29. The three traces are for gauge pressures of 58.3, 92.9, and 162.1 kPa. The zero position is with the piston midstroke in the cylinder, positive values are with the piston higher than midstroke, and negative values are below midstroke. A decrease in capacitance at high and low positions means that the gap is larger; since for PG29 (see Fig. 1) the piston engagement is constant versus height, this indicates a change in the cylinder profile. The decrease in capacitance as the pressure increases is due to the gap becoming wider.

Figure 5 shows a plot of C_g versus $p_{in}-p_a$ for PG35, and Fig. 6 shows h versus $p_{in}-p_a$ for the same gauge. The straight line on Fig. 6 is the linear regression fit of the data, whose slope is used to find the distortion coefficient (see below). The error bars in Fig. 6 are the standard uncertainty

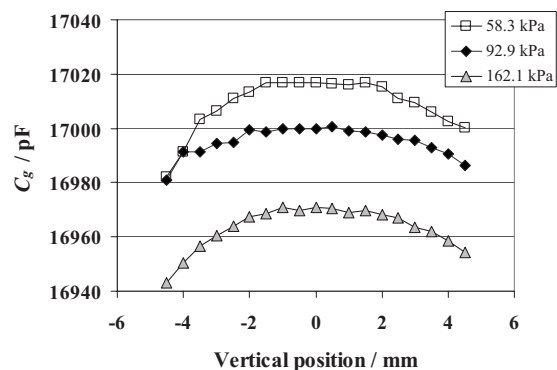


FIG. 4. Gap capacitance as a function of vertical position of piston within cylinder for PG29, at gauge pressures of 58.3, 92.9, and 162.1 kPa.

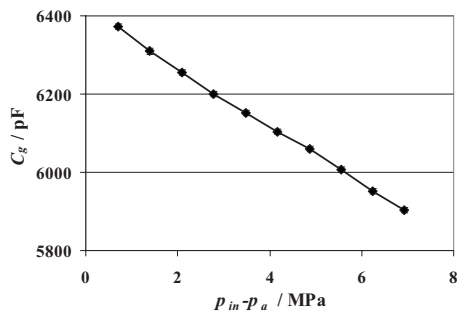


FIG. 5. Capacitance of gap as a function of gauge pressure for PG35.

in the gap, $u(h)$. For all the piston gauges tested, the change in gap with pressure is linear, indicating that the second-order pressure coefficient of Eq. (2) was negligible.

As the pressure range increases, the relative significance of the gap change due to pressure also increases. PG35 (high range gauge) had a 10.3% increase in the gap width over the tested pressure range; PG28 (low range gauge) had a 0.3% increase in the gap over the tested pressure range. Gauges of the same pressure range have similar gaps and similar changes in gap from low to high pressure.

V. CALCULATION OF DISTORTION COEFFICIENT, b_1

Using the approximation that A_e is the average of the piston cross-sectional area and the cylinder cross-sectional area (which is strictly valid only for a straight and round piston and cylinder), for the case when b_2 is zero, it can be shown that¹

$$b_1 = \frac{1}{r} \left(\frac{\partial r_p}{\partial p} + \frac{\partial r_c}{\partial p} \right). \quad (8)$$

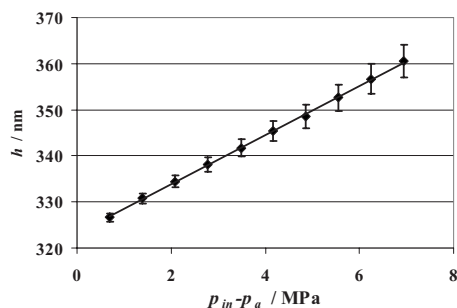
Here, r is the mean radius between the piston radius, r_p , and the cylinder radius, r_c . Using the definition of $h = r_c - r_p$, the cylinder radius can be eliminated from Eq. (8) to give

$$b_1 = \frac{1}{r_p} \left(2 \frac{\partial r_p}{\partial p} + \frac{\partial h}{\partial p} \right). \quad (9)$$

Because the distortion term in Eq. (2) is much less than 1, there is no loss in accuracy in using r_p in place of r . Equation (9) can be written symbolically as

$$b_1 = 2b_p + b_h, \quad (10)$$

with

FIG. 6. Gap clearance in nm as a function of gauge pressure for PG35. Error bars are standard uncertainty in gap, $u(h)$.

$$b_p = \frac{1}{r_p} \frac{\partial r_p}{\partial p}, \quad (11)$$

$$b_h = \frac{1}{r_p} \frac{\partial h}{\partial p}.$$

b_p is the relative change in effective area due to the change in piston radius and b_h is the relative change in effective area due to the change in the clearance gap. The change in piston radius with pressure is calculated analytically using linear elasticity theory; the piston is modeled as being uniformly loaded at the ends at p and loaded uniformly in the gap at $p/2$. Similar modeling of the cylinder shows the piston distortion to be five to ten times smaller than the cylinder distortion. For all the NIST pistons listed in Table I, $b_p = -2.86 \times 10^{-13} \text{ Pa}^{-1}$.

The gap, determined from the capacitance measurements, is fit to a straight line versus pressure, and the linear term of the fit gives $\partial h / \partial p$. Table II summarizes b_h and b_1 from the capacitance method. Also listed are values of b_1 calculated analytically by applying linear elasticity theory to both the piston and the cylinder. Values of b_1 from the capacitance method are comparable to those calculated analytically for the low range gauges, and are larger than values calculated analytically for the middle and high range gauges. When linear elasticity theory is used to calculate b_1 , gauges of the same range have the same distortion since their nominal dimensions and boundary conditions are the same. The capacitive method can distinguish differences in gap distortion, and therefore distortion in effective area, for gauges of the same range. In the far-right column of Table II we list the change in effective area of the piston gauges at the maximum operating pressure, using b_1 calculated from the capacitance measurements. Changes in relative effective area less than 5×10^{-6} are less than the stated standard uncertainty of these gauges. Hence, the capacitance method indicates that distortion is important in determining the effective area of the high range gauges, and less so for the middle and low range gauges.

VI. UNCERTAINTIES

The uncertainty in the gap, h , is found using methods described in Ref. 10. Unless otherwise stated, all uncertainties refer to standard ($k=1$) uncertainties. Uncertainties include both type A components (those evaluated by statistical methods) and type B components (those evaluated by other methods). The measurement equation for h used in evaluating the uncertainty comes from substituting Eq. (7) for the capacitance into Eq. (4) for the gap,

$$h = \frac{\pi DLK \varepsilon_0}{C_T - C_s}. \quad (12)$$

The standard uncertainty in h , or $u(h)$, is found by applying the law of propagation of uncertainty to Eq. (12). Assuming no correlation between the input estimates in Eq. (12), the combined standard uncertainty in h is the square root of the estimated variance, or

TABLE II. Distortion coefficient, standard uncertainty of distortion coefficient, and change in effective area due to distortion at maximum pressure, for six NIST gas piston gauges. p_{\max} is a “gauge” pressure.

Piston gauge	Analytical		Based on capacitance measurements				
	$10^{12} \times b_1$ (Pa ⁻¹)	$10^{12} \times b_h$ (Pa ⁻¹)	$10^{12} \times b_1$ (Pa ⁻¹)	$10^{12} \times u(b_1)$ (Pa ⁻¹)	$u(b_1)/b_1$	p_{\max} (kPa)	$b_1 p_{\max} \times 10^6$
PG28	2.74	3.45	2.88	1.07	0.37	300	0.9
PG29	2.74	4.07	3.50	1.40	0.40	300	1.0
PG34	1.27	2.50	1.93	0.27	0.14	1400	2.7
PG37	1.27	2.47	1.90	0.39	0.21	1400	2.7
PG13	1.02	2.46	1.88	0.55	0.29	7000	13.2
PG35	1.02	3.27	2.70	0.33	0.12	7000	18.9

$$\begin{aligned}
 u_c^2(h) &= \sum_{i=1}^N \left[\frac{\partial h}{\partial x_i} \right]^2 u^2(x_i) \\
 &= \left[\frac{\partial h}{\partial D} \right]^2 u^2(D) + \left[\frac{\partial h}{\partial L} \right]^2 u^2(L) + \left[\frac{\partial h}{\partial K} \right]^2 u^2(K) \\
 &\quad + \left[\frac{\partial h}{\partial C_T} \right]^2 u^2(C_T) + \left[\frac{\partial h}{\partial C_s} \right]^2 u^2(C_s). \quad (13)
 \end{aligned}$$

The partial derivatives are the sensitivity coefficients and the $u(x_i)$ are the standard uncertainties in the inputs. Type A uncertainty is due to the resolution of the measured capacitance using the bridge and is taken as $u_A(C_T) = 1$ pF. All other uncertainties are type B components.

The relative standard uncertainty in D , $u(D)/D$, is taken as 1×10^{-5} . The standard uncertainty in L , $u(L)$, is taken as 0.05 mm. The standard uncertainty in K , $u(K)$, is due to the uncertainty in the appropriate pressure to use in calculating K in Eq. (5). As noted previously, the pressure changes along the engagement position and we currently estimate it assuming that the gap width is constant. We take $u(p)$ as $p_{\text{in}}/4$ and apply the method of Eq. (13) to Eq. (5) for $u(K)$. Type B uncertainty in C_T includes the uncertainty of the calibration of the capacitance bridge, which we take as 3 pF. The agreement with the standard capacitors is better than 3 pF; however, the bridge was used beyond the capacitance values of the standard capacitors and this uncertainty reflects that lack of knowledge in the calibration. For $u(C_T)$ we also include a repeatability component in the capacitance measurement, which represents our ability to repeat the setup that finds the minimum capacitance using the two aforementioned criteria: (1) location of the piston angular position relative to the cylinder and (2) the location of the trim mass on the mass stack. This uncertainty component is estimated as $0.0064C_T$, which comes from evaluating multiple scans of PG34. It is assumed that other piston gauges will have the same relative uncertainty in this component as PG34. Finally, for the uncertainty in the stray capacitance, $u(C_s)$, we estimate the standard uncertainty as 10% of the measured value, or $u(C_s) = 0.1C_s$.

The standard uncertainties for the various piston gauges are summarized in Table I. $u(C_g)$, given in the third column from the far right, is the sum in quadrature of the $u(C_T)$ and $u(C_s)$ components. $u(h)$ is given in the far-right column. For the low range gauges (PG28 and PG29), the largest compo-

nent on a relative basis is the uncertainty in length. $u(h)$ was about 2 nm and does not vary much with pressure. For the midrange gauges (PG34 and PG37), the uncertainty in length is the largest component at low pressure and the uncertainty in K becomes important for 1 MPa and above. Note that PG37 was tested to a lower maximum pressure than PG34. For the high range gauges, the uncertainty increases from 1 nm when the pressure is less than 1 MPa to 3.6 nm at the high pressure; the increase in uncertainty is due to the uncertainty in K at the high pressure.

Similar methods are applied to find the standard uncertainty in the distortion coefficient, $u(b_1)$. The combined uncertainty includes components from b_p , the piston distortion estimated from linear elasticity theory, and from b_h , the gap distortion from the change in gap with pressure. $u(b_p)$ is taken as $0.1b_p$, which will include uncertainties in the elasticity theory and elastic properties of the piston. To determine $u(b_h)$, we look at the measurement equation for b_h [Eq. (11)],

$$b_h = \frac{1}{r_p} \frac{dh}{dp} = 2\pi L \epsilon_0 \frac{d\left(\frac{K}{C_g}\right)}{dp} = 2\pi L \epsilon_0 \left[\frac{1}{C_g} \frac{dK}{dp} - \frac{K}{C_g^2} \frac{dC_g}{dp} \right]. \quad (14)$$

Although we calculate b_h by taking the slope of h versus p , Eq. (14) shows the dependence on the input parameters. We approximate the derivatives in Eq. (14) by the finite differences between the high and low pressures for which the capacitance is measured, for each piston gauge, to evaluate the uncertainty,

$$b_h \approx 2\pi L \epsilon_0 \left[\frac{1}{C_g} \frac{\Delta K}{\Delta p} - \frac{K}{C_g^2} \frac{\Delta C_g}{\Delta p} \right]. \quad (15)$$

When the law of propagation of uncertainty is applied to Eq. (15), by far the largest components on a relative basis are the uncertainties in the *change* in K with pressure and the change in C_g with pressure. Uncertainties in L and Δp are at least an order of magnitude smaller and are ignored. Type B uncertainty in b_h is calculated from the variance,

$$u_B^2(b_h) = \left[\frac{\partial b_h}{\partial \Delta K} \right]^2 u^2(\Delta K) + \left[\frac{\partial b_h}{\partial \Delta C_g} \right]^2 u^2(\Delta C_g). \quad (16)$$

The uncertainty in ΔK is the sum in quadrature of the uncertainty in K at the low and high pressures, which results from the uncertainty of the appropriate pressure to use in the correlation for K . The uncertainty in C_g is the sum in quadrature of the uncertainty in C_g at the low and high pressures; however, we do not include all the components that contributed to $u(C_T)$ in Eq. (13). Specifically, when subtracting the two capacitance values, the stray capacitance is the same in most cases and cancels out; hence the uncertainty due to C_s is not included. The final component of uncertainty in b_1 is type A uncertainty in b_h , which is taken as the uncertainty of the fitted slope. This component ranges from 0.01 to 0.05 of b_1 .

The uncertainties in b_1 for the various piston gauges are summarized in Table II. For the low range gauges, the uncertainty due to capacitance is the largest component, while for the high range gauges the uncertainty in gas permittivity due to the pressure is the largest component. The relative uncertainty $[u(b_1)/b_1]$ varies from 0.12 to 0.40. On a relative basis, the uncertainty is highest for the low range gauges because the change in capacitance with pressure is small compared to the uncertainty in the capacitance measurement.

VII. CONCLUSION

In this work we describe a technique using a capacitance measurement to provide an estimate of the radial gap between a piston and cylinder in a gas piston gauge. This technique can be applied from atmospheric pressure to the highest operating pressure of the gauge, thus providing a measure of the gap with pressure. From the change in gap with pressure we can calculate the distortion coefficient in the effective area of a piston gauge. We use this technique on nonrotating pistons, first finding the angular position of the piston relative to the cylinder that yields a minimum capacitance, and then adjusting a small trim mass (typically 2 g) on the mass stack to yield a further minimum in capacitance. The

assumption is that a minimum in capacitance represents a condition where the piston is centered in the cylinder, or at least where the gap between the piston and cylinder is as large as possible around the circumference.

Calculation of the gap in this manner assumes that the gap is uniform and that a single pressure from inlet to outlet can be used to estimate the gas permittivity. It is likely that these assumptions are not valid, however, even with the restrictions of the method we are able to calculate differences in gap and distortion between similarly designed piston gauges. It is well known, through direct comparison in a pressure cross float experiment, that similarly designed pistons will differ in their distortion coefficients.³ We have estimated the uncertainty of the gap and distortion within the confines of their definition, i.e., no attempt has been made to estimate how the uncertainties would change if the gap varied with angular or vertical position along the piston.

ACKNOWLEDGMENTS

The authors gratefully acknowledge the assistance of R. G. Driver and J. W. Schmidt throughout the project.

¹R. S. Dadson, S. L. Lewis, and G. N. Peggs, *The Pressure Balance: Theory and Practice* (Her Majesty's Stationery Office, London, 1982).

²J. W. Schmidt, K. Jain, A. P. Miiller, W. J. Bowers, and D. A. Olson, *Metrologia* **43**, 53 (2006).

³D.A. Olson, NIST Special Publication No. 250-39, 2009.

⁴NIST Test No. 821/276366-08, 2008.

⁵K. Jain, Y.-C. Cen, W. J. Bowers, and J. W. Schmidt, *J. Res. Natl. Inst. Stand. Technol.* **108**, 11 (2003).

⁶K. Jain, W. J. Bowers, and J. W. Schmidt, *J. Res. Natl. Inst. Stand. Technol.* **108**, 135 (2003).

⁷N. Moiso, I. Severn, and D. R. Sumner, *Metrologia* **42**, S242 (2005).

⁸Certain commercial entities, equipment, or materials may be identified in this document in order to describe an experimental procedure or concept adequately. Such identification is not intended to imply recommendation or endorsement by the National Institute of Standards and Technology, nor is it intended to imply that the entities, materials, or equipment are necessarily the best available for the purpose.

⁹J. S. Schmidt and M. R. Moldover, *Int. J. Thermophys.* **24**, 375 (2003).

¹⁰B. N. Taylor and C. E. Kuyatt, NIST Technical Note No. 1297, 1994.